The Heteronuclear Cluster Chemistry of the Group IB Metals. Part 16.[1] Metal Exchange Reactions in Group IB Metal Heteronuclear Cluster Compounds. Synthesis and Structural Characterization of the Trimetallic Hexanuclear Cluster Compounds $[MM'Ru_4(\mu_3\text{-}H)_2\{\mu\text{-}Ph_2P(CH_2)_nPPh_2\}(CO)_{12}]$ (M = Cu, M' = Ag or Au; M = Ag, M' = Au; $n = 1$ or 2) and X-Ray Crystal Structure of $[AuCuRu_4(\mu_3\text{-}H)_2\{\mu\text{-}Ph_2P(CH_2)_2PPh_2\}(CO)_{12}]$ *

Scott S. D. Brown,[a] **Ian D. Salter**[a] **and Trushar Adatia**[b]
[a] *Department of Chemistry, University of Exeter, Exeter EX4 4QD, UK*
[b] *School of Chemistry, University of North London, London N7 8DB, UK*

Treatment of dichloromethane solutions of the heteronuclear cluster compounds $[M_2Ru_4(\mu_3\text{-}H)_2\{\mu\text{-}Ph_2P(CH_2)_nPPh_2\}(CO)_{12}]$ (M = Cu or Ag, $n = 1$ or 2) with dichloromethane solutions containing the appropriate quantities of the complex $[Ag(NCMe)_4]PF_6$ or $[AuCl(SC_4H_8)]$ results in the replacement of either one or both of the Group IB metals M by silver or gold atoms. The products from these Group IB metal exchange reactions are obtained in *ca.* 65–75% yield. The synthetic approach is especially useful for the preparation of the novel trimetallic species $[MM'Ru_4(\mu_3\text{-}H)_2\{\mu\text{-}Ph_2P(CH_2)_nPPh_2\}(CO)_{12}]$ (M = Cu, M' = Ag or Au; M = Ag, M' = Au; $n = 1$ or 2). These clusters have all been characterized by IR and NMR spectroscopy and the structure of $[AuCuRu_4(\mu_3\text{-}H)_2\{\mu\text{-}Ph_2P(CH_2)_2PPh_2\}(CO)_{12}]$ has been determined by a single-crystal X-ray diffraction study. The spectroscopic data show that all of the clusters in the series adopt similar structures. The metal framework consists of a tetrahedron of ruthenium atoms, with one face capped by a Group IB metal and one of the MRu_2 faces of the MRu_3 tetrahedron so formed further capped by the second Group IB metal, to give an overall capped trigonal-bipyramidal metal core geometry. The other two MRu_2 faces are both capped by a triply bridging hydrido ligand and the bidentate diphosphine ligand bridges the two coinage metals. Each ruthenium atom is ligated by three essentially linear CO groups. In each case, the lighter of the pair of Group IB metals occupies the site of higher co-ordination number and the heavier is in the position of lower co-ordination number. Interestingly, variable-temperature NMR spectroscopic studies show that the metal frameworks of $[MM'Ru_4(\mu_3\text{-}H)_2\{\mu\text{-}Ph_2P(CH_2)_nPPh_2\}(CO)_{12}]$ are stereochemically rigid in solution at ambient temperature, in marked contrast to the dynamic behaviour involving intramolecular coinage-metal site-exchange, which has been previously reported for analogous bimetallic species.

The chemistry of transition-metal cluster compounds containing one or more $M(PR_3)$ (M = Cu, Ag or Au; R = alkyl or aryl) units bonded to other, different transition metals has attracted a great deal of recent interest.[2,3] In contrast to the majority of currently known preparative routes to other types of mixed-metal cluster compound, in which chance still normally plays an important role,[4] the study of heteronuclear Group IB metal clusters has greatly benefited from the availability of a number of generally applicable rational procedures for their synthesis in high yield.[2,3] The vast majority of these synthetic routes increase the cluster nuclearity by incorporating $M(PR_3)$ fragments into a preformed cluster, dimer or monomer.[2,3] However, Group IB metal exchange reactions, in which the complexes $[M'X(PPh_3)]$ (M' = Cu or Au, X = Cl; M' = Ag, X = I) are utilized to replace one or two $M(PPh_3)$ units in a mixed-metal cluster compound by similar fragment(s) containing the different coinage metal M', with no overall change in the cluster nuclearity, have recently been reported as a novel alternative preparative method.[5,6] These metal exchange reactions are of particular interest because they provide a useful route to heteronuclear cluster compounds containing two different coinage metals, which are very rare at present.[2,6,7] Unfortunately, the synthetic approach is currently restricted to exchanging $M(PR_3)$ groups and it cannot be applied to compounds such as the series of hexanuclear clusters $[M_2Ru_4H_2\{\mu\text{-}Ph_2E(CH_2)_nE'Ph_2\}(CO)_{12}]$ (M = Cu, Ag or Au; E = E' = P, n = 1–6; E = As, E' = As or P, n = 1 or 2),[8–11] in which the bidentate ligands bridge the two coinage metals. However, we anticipated that mononuclear Group IB metal complexes, in which the ligands are labile, would be more generally applicable reagents for coinage-metal exchange reactions with cluster compounds. In addition, it has been previously reported[5,6] that Group IB metal exchange reactions are more efficient when the lighter of the pair or pairs of coinage metals to be exchanged is initially present in the cluster compound than *vice versa*. Therefore, we decided to investigate the effect of treating the bimetallic species $[M_2Ru_4(\mu_3\text{-}H)_2\{\mu\text{-}Ph_2P(CH_2)_nPPh_2\}(CO)_{12}]$ (M = Cu or Ag, $n = 1$ or 2) with the complexes $[Ag(NCMe)_4]PF_6$ and $[AuCl(SC_4H_8)]$. A preliminary account describing some of our results has already been published.[12]

---

* *Supplementary data available:* see Instructions for Authors, *J. Chem. Soc., Dalton Trans.*, 1993, Issue 1, pp. xxiii–xxviii.

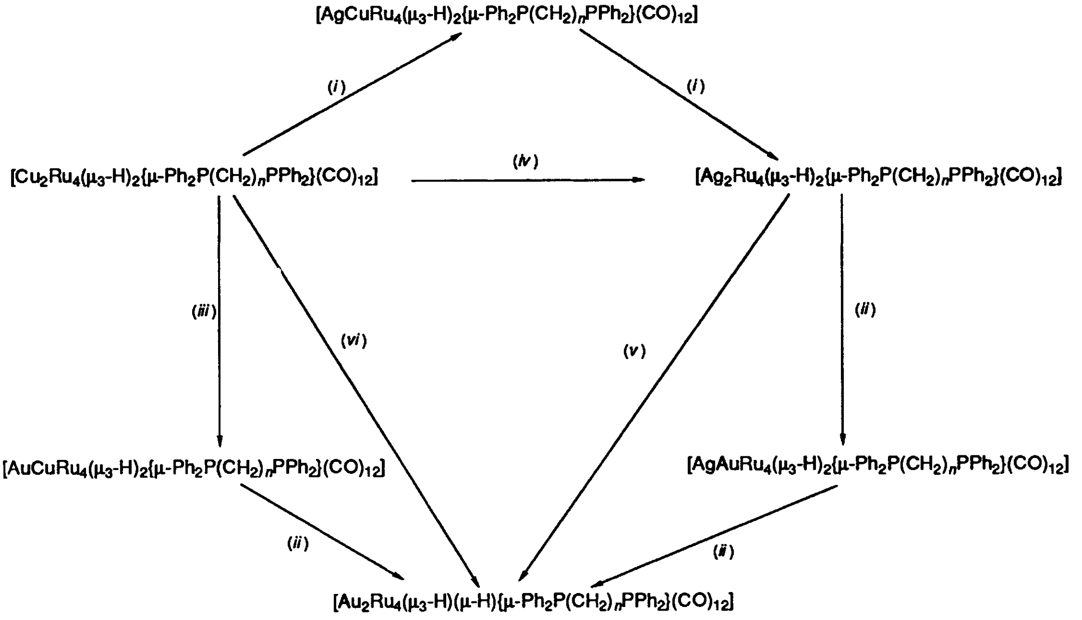

Scheme 1 Summary of the Group IB metal exchange reactions. (*i*) $[Ag(NCMe)_4]PF_6$ (1.5 equiv.), (*ii*) $[AuCl(SC_4H_8)]$ (1 equiv.), (*iii*) $[AuCl(SC_4H_8)]$ (0.9 equiv.), (*iv*) $[Ag(NCMe)_4]PF_6$ (3 equiv.), (*v*) $[AuCl(SC_4H_8)]$ (2.3 equiv.), (*vi*) $[AuCl(SC_4H_8)]$ (2.1 equiv.)

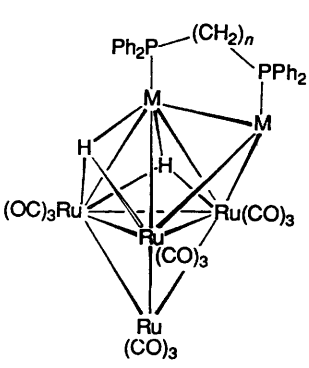

	M	*n*
1	Cu	1
2	Cu	2
3	Ag	1
4	Ag	2

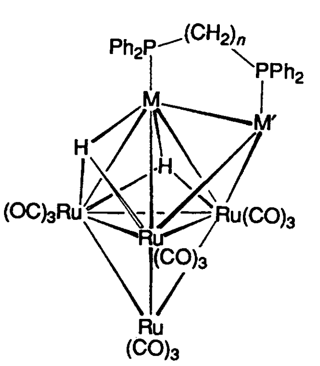

	M	M′	*n*
5	Cu	Ag	1
6	Cu	Ag	2
7	Cu	Au	1
8	Cu	Au	2
9	Ag	Au	1
10	Ag	Au	2

Results and Discussion

Treatment of dichloromethane solutions of the previously reported[8] bimetallic species $[M_2Ru_4(\mu_3\text{-}H)_2\{\mu\text{-}Ph_2P(CH_2)_nPPh_2\}(CO)_{12}]$ (M = Cu, *n* = 1 **1** or 2 **2**; M = Ag, *n* = 1 **3** or 2 **4**) with dichloromethane solutions containing the appropriate amounts of the compound $[Ag(NCMe)_4]PF_6$ or $[AuCl(SC_4H_8)]$ results in the replacement of either one or both of the Group IB metals present in the cluster by the coinage metal contained in the mononuclear complex, as shown in Scheme 1. The syntheses of the trimetallic clusters $[MM'Ru_4(\mu_3\text{-}H)_2\{\mu\text{-}Ph_2P(CH_2)_nPPh_2\}(CO)_{12}]$ (M = Cu, M′ = Ag, *n* = 1 **5** or 2 **6**; M = Cu, M′ = Au, *n* = 1 **7** or 2 **8**; M = Ag, M′ = Au, *n* = 1 **9** or 2 **10**) also produce very small amounts of a bimetallic cluster, in which both of the Group IB metals initially present in the starting material have been replaced. When the trimetallic clusters **5**–**10** are treated with the complex $[Ag(NCMe)_4]PF_6$ or $[AuCl(SC_4H_8)]$, the lighter of the two Group IB metals is replaced to afford bimetallic species (Scheme 1). The yields for all of these reactions lie in the range *ca.* 65–75%.

The bimetallic species $[Au_2Ru_4(\mu_3\text{-}H)(\mu\text{-}H)\{\mu\text{-}Ph_2P(CH_2)_nPPh_2\}(CO)_{12}]$ (*n* = 1 **11** or 2 **12**) have been previously prepared *via* an alternative route, which involved treating the salt $[N(PPh_3)_2]_2[Ru_4(\mu\text{-}H)_2(CO)_{12}]$ with the appropriate complex $[Au_2\{\mu\text{-}Ph_2P(CH_2)_nPPh_2\}Cl_2]$, in the presence of $TlPF_6$.[9,11] The ^1H and $^{31}P\text{-}\{^1H\}$ NMR and IR spectra of samples of the silver-containing bimetallic clusters **3** and **4** and the gold-containing species **11** and **12**, which were prepared *via* the metal exchange reactions described herein, are identical to the data quoted in the literature.[8,9,11]

Although bimetallic clusters can be obtained from the above Group IB metal exchange reactions, this synthetic approach is potentially much more useful for the preparation of trimetallic species, which remain relatively rare[2] and which are much less readily synthesised by the direct addition of coinage-metal fragments to cluster anions than bimetallic clusters.[5,6] The unusual trimetallic clusters $[AuMRu_4(\mu_3\text{-}H)_2\{\mu\text{-}Ph_2P(CH_2)_nPPh_2\}(CO)_{12}]$ (M = Cu, *n* = 1 **7** or 2 **8**; M = Ag, *n* = 1 **9** or 2 **10**) have not been reported previously and they were characterized by microanalyses and by spectroscopic measurements (Tables 1 and 2). This set of data is entirely consistent with the proposed formulations. The synthesis of the clusters $[AgCuRu_4(\mu_3\text{-}H)_2\{\mu\text{-}Ph_2P(CH_2)_nPPh_2\}(CO)_{12}]$ (*n* = 1 **5** or 2 **6**) *via* an alternative route, which involved treating the salt $[N(PPh_3)_2]_2[Ru_4(\mu\text{-}H)_2(CO)_{12}]$ with a mixture containing 1 equivalent of $[Cu(NCMe)_4]PF_6$ and 1 equivalent of $[Ag(NCMe)_4]PF_6$, followed by the addition of 1 equivalent of the appropriate bidentate diphosphine ligand, has been very briefly mentioned in a preliminary communication.[13] However, no analytical or spectroscopic data for **5** and **6** have appeared in the literature, so this information is also presented in Tables 1 and 2. The ^1H and $^{31}P\text{-}\{^1H\}$ NMR and IR spectra of samples of the trimetallic species **5** and **6**, which were synthesised *via* the original route,[14] are identical to those of samples prepared *via* the Group IB metal exchange reactions described herein.

The IR and NMR spectra of the trimetallic clusters **5**–**10** are closely similar to those previously reported[6] for the analogous PPh_3-ligated species $[MM'Ru_4(\mu_3\text{-}H)_2(CO)_{12}(PPh_3)_2]$ (M = Cu, M′ = Ag **13** or Au **14**; M = Ag, M′ = Au **15**), which implies that clusters **5**–**10** all adopt similar capped trigonal-bipyramidal metal framework geometries to those established for **13**–**15**. However, to investigate the structure of one of the novel $Ph_2P(CH_2)_nPPh_2$-containing trimetallic clusters **5**–**10** in detail, a single-crystal X-ray diffraction study was performed on

Table 1 Analytical[a] and physical data for the new Group IB metal heteronuclear cluster compounds[b]

Cluster compound	M.p. (θ_c/°C) (decomp.)	ν_{max}(CO)[c]/cm^{-1}	Analysis (%) C	Analysis (%) H
5 $[AgCuRu_4(\mu_3\text{-}H)_2(\mu\text{-}Ph_2PCH_2PPh_2)(CO)_{12}]$	155–159	2071s, 2034vs, 2018vs, 2010 (sh), 1969m (br), 1929w (br)	33.8 (34.2)	1.9 (1.8)
6 $[AgCuRu_4(\mu_3\text{-}H)_2\{\mu\text{-}Ph_2P(CH_2)_2PPh_2\}(CO)_{12}]$	177–181	2070s, 2033vs, 2020vs, 2004s, 1976m (br), 1935w (br)	34.7 (34.8)	2.2 (2.0)
7 $[AuCuRu_4(\mu_3\text{-}H)_2(\mu\text{-}Ph_2PCH_2PPh_2)(CO)_{12}]$	184–188	2072s, 2037vs, 2021vs, 2010 (sh), 1976m, (br), 1938w (br)	31.8 (32.0)	1.6 (1.7)
8 $[AuCuRu_4(\mu_3\text{-}H)_2\{\mu\text{-}Ph_2P(CH_2)_2PPh_2\}(CO)_{12}]$	170–174	2071s, 2035vs, 2022vs, 2009s, 1979m (br), 1948w (br)	32.6 (32.6)	2.0 (1.9)
9 $[AgAuRu_4(\mu_3\text{-}H)_2(\mu\text{-}Ph_2PCH_2PPh_2)(CO)_{12}]$	179–183	2070s, 2036vs, 2020s, 2009 (sh), 1970m (br), 1935w (br)	30.7 (31.0)	1.9 (1.7)
10 $[AgAuRu_4(\mu_3\text{-}H)_2\{\mu\text{-}Ph_2P(CH_2)_2PPh_2\}(CO)_{12}]$	163–167	2070s, 2034vs, 2020s, 2007s, 1970m (br), 1939w (br)	31.2 (31.6)	1.9 (1.8)

[a] Calculated values given in parentheses. [b] The synthesis of the clusters $[AgCuRu_4(\mu_3\text{-}H)_2\{\mu\text{-}Ph_2P(CH_2)_nPPh_2\}(CO)_{12}]$ ($n = 1$ or 2) *via* an alternative route, which involved treating the salt $[N(PPh_3)_2]_2[Ru_4(\mu\text{-}H)_2(CO)_{12}]$ with a mixture of 1 equivalent of $[Cu(NCMe)_4]PF_6$ and 1 equivalent of $[Ag(NCMe)_4]PF_6$, followed by the addition of 1 equivalent of $Ph_2P(CH_2)_nPPh_2$, has been very briefly mentioned in a preliminary communication.[13] However, no analytical or spectroscopic data were reported. [c] Measured in dichloromethane solution.

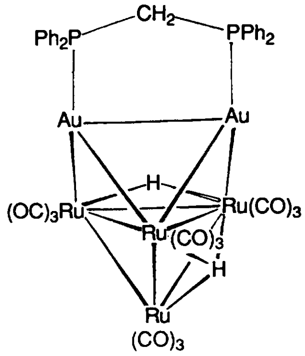

11

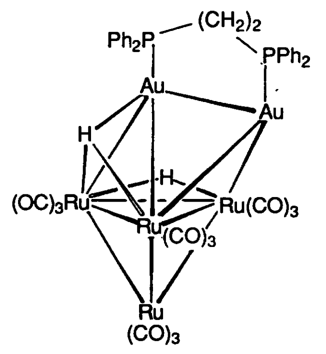

12

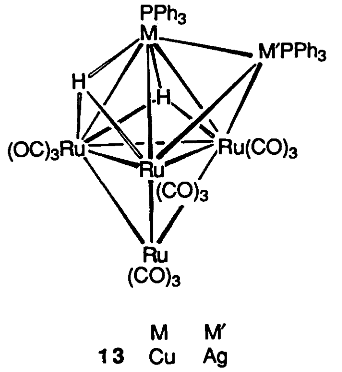

	M	M′
13	Cu	Ag
14	Cu	Au
15	Ag	Au

$[AuCuRu_4(\mu_3\text{-}H)_2\{\mu\text{-}Ph_2P(CH_2)_2PPh_2\}(CO)_{12}]$ **8**. Discussion of the NMR spectroscopic data of **5**–**10** is best deferred until the X-ray diffraction results have been presented.

The molecular structure of $[AuCuRu_4(\mu_3\text{-}H)_2\{\mu\text{-}Ph_2P(CH_2)_2PPh_2\}(CO)_{12}]$ is illustrated in Fig. 1, which also shows the crystallographic numbering scheme. Selected bond lengths and bond angles are presented in Table 3. The metal skeleton of **8** consists of a tetrahedron of ruthenium atoms, with one face [Ru(1)Ru(3)Ru(4)] capped by a copper atom [Group IB metal site M(2)] and one of the faces of the $CuRu_3$ tetrahedron so formed further capped by a gold atom [Group IB metal site M(1)], to give an overall capped trigonal-bipyramidal metal core geometry. The bidentate diphosphine ligand bridges the Au–Cu vector and the Ru atoms are all ligated by three terminal CO groups, which are essentially linear. The two hydrido ligands cap the CuRu(1)Ru(3) and CuRu(1)Ru(4) faces of the cluster.

Fig. 2 compares the bond lengths within the metal framework of **8** with the metal–metal separations in the analogous bimetallic clusters $[M_2Ru_4H_2\{\mu\text{-}Ph_2P(CH_2)_2PPh_2\}(CO)_{12}]$ (M = Cu **2** or Au **12**). In general, the metal–metal distances in the trimetallic species **8** are reasonably similar to the equivalent separations in the appropriate bimetallic analogue. Within the above three clusters, relatively small differences in the equivalent distances between the Group IB metals and the ruthenium atoms are to be expected, since the relative 'softness' of this type of metal–metal bonding is well established.[2,3] For example, Fig. 2 shows the significant differences observed[8] between some of the equivalent metal–metal separations in the two independent molecules, which occur in the asymmetric unit of the copper-containing species **2**, and crystal packing forces are known[11] to cause differences of up to 0.091 Å between the equivalent Au–Ru distances in the metal frameworks of the two crystalline modifications of $[Au_2Ru_4(\mu_3\text{-}H)(\mu\text{-}H)(\mu\text{-}Ph_2PCH_2PPh_2)(CO)_{12}]$ **11**. The Au–Cu distance in **8** [2.614(2) Å] is intermediate between the mean of the two Cu–Cu separations observed for the two independent molecules in the asymmetric unit of **2** [2.499(3) Å][8] and the length of the Au–Au vector in **12** [2.828(4) Å].[11] In all three cluster compounds, the Ru–Ru vectors, which are bridged by the Group IB metals, are significantly longer than the unbridged Ru–Ru separations in the Ru_4 tetrahedra, as expected.

Three short contacts between the Group IB metals and the carbon atoms of CO ligands occur in **8** [Au•••C(32) 2.70(3), Au•••C(42) 2.75(3), and Cu•••C(12) 2.57(3) Å]. Although similar short M•••C contacts between coinage metals and essentially linear CO ligands, which are bonded to adjacent metals, are a structural feature of many Group IB metal heteronuclear clusters, the exact nature of this interaction is not well understood.[2]

Previous work on a series of phosphine-ligated bimetallic clusters analogous to **5**–**10** has shown that their capped trigonal-bipyramidal metal skeletons undergo dynamic behaviour involving intramolecular coinage-metal site-exchange at ambient temperature in solution.[1,8–11,15–18] When this dynamic process occurs, the hydrido ligands are observed to couple to two equivalent phosphorus atoms. However, in many cases, it is also possible to observe NMR spectra consistent with the ground-state structures at low temperatures. In these cases, the

Table 2 Hydrogen-1 and phosphorus-31 NMR spectroscopic data[a] for the new Group IB metal heteronuclear cluster compounds[b]

Cluster	^{1}H NMR data[c]	Low-temperature ^{1}H NMR hydrido ligand signal[d]	^{31}P-{^{1}H} NMR data[e]
5	-18.29 [d, 2 H, μ_3-H, *J*(PH) 12], 3.43 [apparent d of t (overlapping d of d of d), 2 H, PCH_2P, *J*(PH) 10, *J*(AgH)$_{av.}$ 3], 7.27–7.48 (m, 20 H, Ph)	-18.31 [d, 2 H, *J*(PH) 11]	2.4 [2 × d of d, 1 P, PAg, *J*(^{109}AgP) 444, *J*(^{107}AgP) 392, *J*(PP) 102], 1.5 [d of d, 1 P, PCu, *J*(PP) 102, *J*(AgP)$_{av.}$ 15]
6	-17.91 [d, 2 H, μ_3-H, *J*(PH) 12], 2.30–2.62 [m, 4 H, $P(CH_2)_2P$], 7.50–7.64 (m, 20 H, Ph)	-17.99 [d, br, 1 H, *J*(PH) 12], -17.83 [d, br, 1 H, *J*(PH) 11]	11.2 [2 × d of d, 1 P, PAg, *J*(^{109}AgP) 465, *J*(^{107}AgP) 403, *J*(PP) 2], 2.9 (s br, 1 P, PCu)
7	-18.89 [d of d, 2 H, μ_3-H, *J*(PH) 14 and 1], 3.63 [apparent t (overlapping d of d), 2 H, PCH_2P, *J*(PH) 11], 7.28–7.57 (m, 20 H, Ph)	-19.12 [d, 2 H, *J*(PH) 14]	60.6 [d, 1 P, PAu, *J*(PP) 69], -4.0 [d, 1 P, PCu, *J*(PP) 69]
8	-18.12 [d, 2 H, μ_3-H, *J*(PH) 13], 2.34–2.65 [m, 4 H, $P(CH_2)_2P$], 7.35–7.62 (m, 20 H, Ph)	-18.26 [d, 1 H, *J*(PH) 13], -18.05 [d, 1 H, *J*(PH) 12]	69.6 (s, 1 P, PAu), 4.5 (s, br, 1 P, PCu)
9	-18.15 [2 × d of d of d, 2 H, μ_3-H, *J*(^{109}AgH) 38, *J*(^{107}AgH) 33, *J*(PH) 12 and 2], 3.69 [apparent d of t (overlapping d of d of d), 2 H, PCH_2P, *J*(PH) 11, *J*(AgH)$_{av.}$ 5], 7.28–7.57 (m, 20 H, Ph)	-18.44 [d of d, 2 H, *J*(AgH)$_{av.}$ 37, *J*(PH) 13]	59.1 [d of d, 1 P, PAu, *J*(PP) 75, *J*(AgP)$_{av.}$ 12], 3.7 [2 × d of d, 1 P, PAg, *J*(^{109}AgP) 610, *J*(^{107}AgP) 529, *J*(PP) 75]
10	-17.66 [2 × d of d of d, 2 H, μ_3-H, *J*(^{109}AgH) 39, *J*(^{107}AgH) 34, *J*(PH) 11 and 1], 2.46–2.71 [m, 4 H, $P(CH_2)_2P$], 7.51–7.72 (m, 20 H, Ph)	[f] *ca.* -17.8 [d of d, br, 1 H, *J*(AgH)$_{av.}$ *ca.* 37, *J*(PH) *ca.* 9], *ca.* -17.6 [d of d br, 1 H, *J*(AgH)$_{av.}$ *ca.* 38, *J*(PH) *ca.* 7]	69.6 [d, 1 P, PAu, *J*(AgP)$_{av.}$ 12], 14.2 [2 × d of d, 1 P, *J*(^{109}AgP) 601, *J*(^{107}AgP) 521, *J*(PP) 1]

[a] Chemical shifts (δ) in ppm, coupling constants in Hz. [b] The synthesis of the clusters $[AgCuRu_4(\mu_3\text{-}H)_2\{\mu\text{-}Ph_2P(CH_2)_nPPh_2\}(CO)_{12}]$ (*n* = 1 **5** or 2 **6**) *via* an alternative route, which involved treating the salt $[N(PPh_3)_2]_2[Ru_4(\mu\text{-}H)_2(CO)_{12}]$ with a mixture of 1 equivalent of $[Cu(NCMe)_4]PF_6$ and 1 equivalent of $[Ag(NCMe)_4]PF_6$, followed by the addition of 1 equivalent of $Ph_2P(CH_2)_nPPh_2$, has been very briefly mentioned in a preliminary communication.[13] However, no spectroscopic data were reported. [c] Measured in [$^2H_2$]dichloromethane solution at ambient temperature. [d] Measured in [$^2H_2$]dichloromethane solution at −100 °C. [e] Hydrogen-1 decoupled. Measured in [$^2H_2$]dichloromethane–CH_2Cl_2 solution at −90 °C. Chemical shifts positive to high frequency of 85% H_3PO_4 (external). [f] The two separate hydrido ligand signals overlap, so the chemical shifts and coupling constants, which were measured from the spectrum, are only approximate.

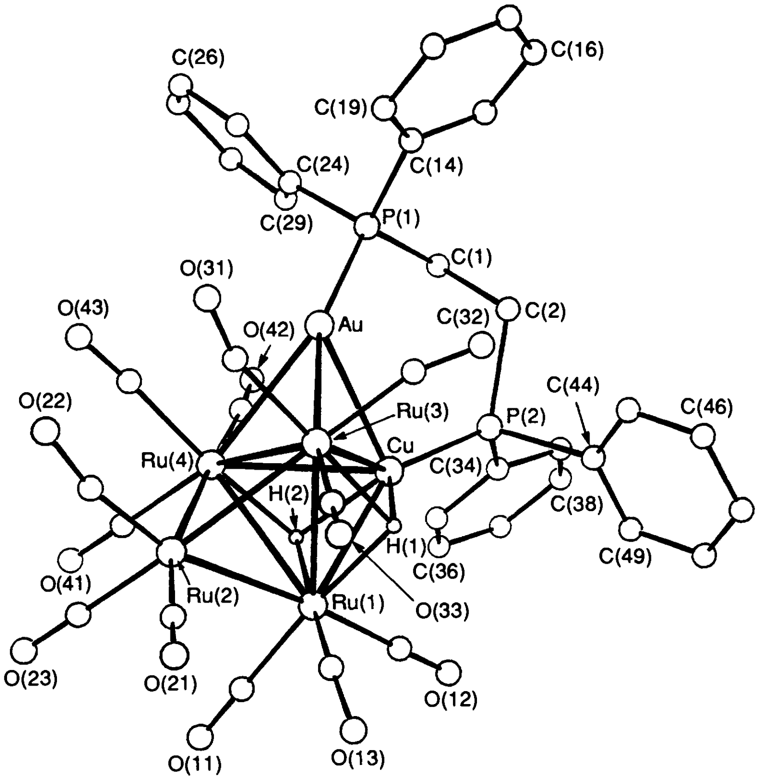

Fig. 1 Molecular structure of $[AuCuRu_4(\mu_3\text{-}H)_2\{\mu\text{-}Ph_2P(CH_2)_2PPh_2\}(CO)_{12}]$ **8**, showing the crystallographic numbering. The carbon atom of each carbonyl group has the same number as the oxygen atom

high-field hydrido ligand signals in the ^{1}H NMR spectra show couplings to the phosphorus atoms attached to the Group IB metals in the site M(2) (Fig. 2) [*J*(PH) 8–14 Hz], but not to those bonded to the coinage metals in position M(1).[1,8,10,16–18] In addition, if a silver atom occupies site M(2), the hydrido ligand signals are split by additional ^{107,109}Ag–^{1}H couplings, but these couplings are not observed for silver atoms in position M(1).[1,8,10,17,18] The high-field hydrido ligand signals in the ^{1}H

Table 3 Selected bond lengths (Å) and angles (°), with estimated standard deviations in parentheses, for $[AuCuRu_4(\mu_3\text{-}H)_2\{\mu\text{-}Ph_2P(CH_2)_2PPh_2\}(CO)_{12}]$ **8**

Au–Cu	2.614(2)	Au–Ru(3)	2.823(2)	Ru(1)–Ru(4)	2.930(3)	Ru(2)–Ru(3)	2.815(3)
Au–Ru(4)	2.823(2)	Au–P(1)	2.21(3)	Ru(2)–Ru(4)	2.813(3)	Ru(3)–Ru(4)	2.964(3)
Cu–Ru(1)	2.674(3)	Cu–Ru(3)	2.817(3)	P(1)–C(1)	1.90(7)	P(1)–C(14)	1.96(7)
Cu–Ru(4)	2.822(3)	Cu–P(2)	2.15(4)	P(1)–C(24)	1.97(7)	P(2)–C(2)	1.88(7)
Ru(1)–Ru(2)	2.803(3)	Ru(1)–Ru(3)	2.985(3)	P(2)–C(34)	1.90(7)	P(2)–C(44)	1.99(7)
C(1)–C(2)	1.81(9)					Range Ru–CO	1.72–1.91(6)
						Range C–O	1.07–1.19(9)
Ru(3)–Au–Cu	62.1(3)	Ru(4)–Au–Cu	62.1(3)	Ru(3)–Ru(2)–Ru(1)	64.1(4)	Ru(4)–Ru(2)–Ru(1)	63.5(4)
Ru(4)–Au–Ru(3)	62.2(3)	P(1)–Au–Cu	114(1)	Ru(4)–Ru(2)–Ru(3)	64.8(4)	Cu–Ru(3)–Au	54.5(6)
P(1)–Au–Ru(3)	160(2)	P(1)–Au–Ru(4)	135(1)	Ru(1)–Ru(3)–Au	103.2(5)	Ru(1)–Ru(3)–Cu	56.4(7)
Ru(1)–Cu–Au	117(1)	Ru(3)–Cu–Au	63.4(5)	Ru(2)–Ru(3)–Au	114.1(7)	Ru(2)–Ru(3)–Cu	104.1(6)
Ru(3)–Cu–Ru(1)	63.7(6)	Ru(4)–Cu–Au	63.8(5)	Ru(2)–Ru(3)–Ru(1)	57.9(6)	Ru(4)–Ru(3)–Au	59.3(5)
Ru(4)–Cu–Ru(1)	63.1(5)	Ru(4)–Cu–Ru(3)	63.1(5)	Ru(4)–Ru(3)–Cu	58.7(5)	Ru(4)–Ru(3)–Ru(1)	59.2(6)
P(2)–Cu–Au	95(2)	P(2)–Cu–Ru(1)	147(2)	Ru(4)–Ru(3)–Ru(2)	57.8(6)	Cu–Ru(4)–Au	54.1(6)
P(2)–Cu–Ru(3)	135(2)	P(2)–Cu–Ru(4)	144(2)	Ru(1)–Ru(4)–Au	103.1(6)	Ru(1)–Ru(4)–Cu	56.5(7)
Ru(2)–Ru(1)–Cu	107.1(5)	Ru(3)–Ru(1)–Cu	59.9(5)	Ru(2)–Ru(4)–Au	113.0(6)	Ru(2)–Ru(4)–Cu	103.5(6)
Ru(3)–Ru(1)–Ru(2)	58.0(4)	Ru(4)–Ru(1)–Cu	60.4(5)	Ru(2)–Ru(4)–Ru(1)	58.0(7)	Ru(3)–Ru(4)–Au	58.5(4)
Ru(4)–Ru(1)–Ru(2)	58.5(4)	Ru(4)–Ru(1)–Ru(3)	61.0(4)	Ru(3)–Ru(4)–Cu	58.2(6)	Ru(3)–Ru(4)–Ru(1)	59.8(6)
Ru(3)–Ru(4)–Ru(2)	57.4(6)						
C(1)–P(1)–Au	116(3)	C(14)–P(1)–Au	104(4)	C(2)–P(2)–Cu	115(4)	C(34)–P(2)–Cu	114(4)
C(14)–P(1)–C(1)	105(7)	C(24)–P(1)–Au	116(4)	C(34)–P(2)–C(2)	97(6)	C(44)–P(2)–Cu	118(4)
C(24)–P(1)–C(1)	95(8)	C(24)–P(1)–C(14)	110(6)	C(44)–P(2)–C(2)	98(8)	C(44)–P(2)–C(34)	85(8)
C(1)–C(2)–P(2)	123(7)	C(2)–C(1)–P(1)	95(5)				

Range of Ru–C–O 168–179(7).

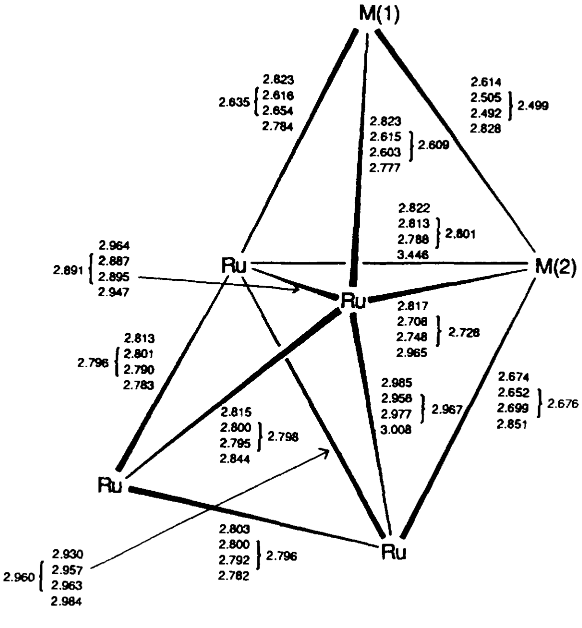

Fig. 2 A comparison of the metal–metal separations (Å) in the metal cores of $[MM'Ru_4H_2\{\mu\text{-}Ph_2P(CH_2)_2PPh_2\}(CO)_{12}]$ (M = Cu, M′ = Au **8**, M = M′ = Cu **2** and M = M′ = Au **12**). [There are two independent molecules (A and B) in the asymmetric unit of **2**.[8]] Distances are given in the following descending order: **8**, molecule A of **2**,[8] molecule B of **2**,[8] and **12**.[11] The single figures adjacent to the brackets are the means of the equivalent separations in molecules A and B of **2**

NMR spectra of **5**–**10** all show a coupling to one phosphorus atom with magnitudes of *J*(PH) in the range 11–14 Hz* (Table 2). Thus, the metal frameworks of the trimetallic clusters **5**–**10** are all stereochemically rigid in solution at ambient temperature, in marked contrast to the intramolecular metal core rearrangements observed for the analogous bimetallic species.[1,8–11,15–18] Similar stereochemical rigidity has been previously reported[6] for the metal cores of the closely related PPh_3-ligated trimetallic clusters **13**–**15**. Interestingly, the high-field hydrido ligand signals in the ^1H NMR spectra of **9** and **10** show $^{107,109}Ag$–^1H couplings, but those in the spectra of the silver-containing clusters **5** and **6** do not. Thus, in each of **5**, **6**, **9** and **10** the lighter of the pair of Group IB metals occupies the site of higher co-ordination number [M(2)] (Fig. 2) and the heavier is in the position of lower co-ordination number [M(1)], as was observed in the X-ray diffraction study of **8** and for the closely related PPh_3-ligated species **13**–**15**.[6] In addition, it seems very likely that the copper and gold atoms in the $Ph_2PCH_2PPh_2$-ligated cluster **7** occupy the same Group IB metal sites as they do in the analogous $Ph_2P(CH_2)_2PPh_2$-containing species **8** and the closely related PPh_3-ligated cluster **14**.[6]

Interestingly, the stereochemical rigidity observed in solution for the metal frameworks of the trimetallic clusters **5**–**10** and **13**–**15**[6] is entirely consistent with recent work by Orpen and Salter.[19] These workers postulated that the pathway for site exchange of gold atoms in cluster compounds containing Au_2Ru_3 fragments involves a partial Berry pseudorotation, in which the geometry of the Au_2Ru_3 unit changes from trigonal bipyramidal *TBPY* to square pyramidal and then back to *TBPY*, with exchange of gold atom environments. This hypothesis was tested against data derived from 16 crystal structures of compounds containing Au_2Ru_3 fragments and the Berry-like mechanism was found to be fully consistent with the structural evidence. However, the two different Group IB metals in the trimetallic clusters cannot exchange by this mechanism, hence no dynamic behaviour involving intramolecular metal core rearrangements occurs for the trimetallic species in solution.

The capped trigonal-bipyramidal skeletal geometries adopted by the gold-containing trimetallic clusters **7**–**10** are interesting in view of the metal framework structures previously established for the analogous bimetallic species **11** and **12**.[11] In the latter two clusters, the capped trigonal-bipyramidal metal core structure, which is almost always preferred by clusters of this general type, has been distorted to a capped square-based pyramid by the $Ph_2PCH_2PPh_2$ ligand in **11** and to a structure

---

* Additional very small ^{31}P–^1H couplings [*J*(PH) 1–2 Hz] were also observed for **7**, **9** and **10**. The couplings are due to the phosphorus atom which is attached to the Group IB metal in site M(1). Therefore, these small couplings through three bonds are also consistent with the proposed stereochemical rigidity of the metal frameworks of **7**, **9** and **10** at ambient temperature in solution.

Table 4 Conditions used and quantities of product obtained for the Group IB metal exchange reactions

(*a*) Synthesis of the trimetallic clusters $[MM'Ru_4(\mu_3\text{-}H)_2\{\mu\text{-}Ph_2P(CH_2)_nPPh_2\}(CO)_{12}]$ (M = Cu, M′ = Ag or Au; M = Ag, M′ = Au; *n* = 1 or 2)

Reagents and quantities (g, mmol) used	Product isolated (yield)[a]
$[Cu_2Ru_4(\mu_3\text{-}H)_2\{\mu\text{-}Ph_2P(CH_2)_nPPh_2\}(CO)_{12}]$ (*n* = 1, 0.30, 0.24; *n* = 2, 0.30, 0.24), $[Ag(NCMe)_4]PF_6$ (0.15, 0.36)	[b,c] $[AgCuRu_4(\mu\text{-}H)_2\{\mu\text{-}Ph_2P(CH_2)_nPPh_2\}(CO)_{12}]$ (*n* = 1, 0.21 g, 68%; *n* = 2, 0.20 g, 64%)
$[Cu_2Ru_4(\mu_3\text{-}H)_2\{\mu\text{-}Ph_2P(CH_2)_nPPh_2\}(CO)_{12}]$ (*n* = 1, 0.30, 0.24; *n* = 2, 0.30, 0.24), $[AuCl(SC_4H_8)]$ (0.07, 0.22)	[d,e] $[AuCuRu_4(\mu_3\text{-}H)_2\{\mu\text{-}Ph_2P(CH_2)_nPPh_2\}(CO)_{12}]$ (*n* = 1, 0.23 g, 69%; *n* = 2, 0.24 g, 72%)
$[Ag_2Ru_4(\mu_3\text{-}H)_2\{\mu\text{-}Ph_2P(CH_2)_nPPh_2\}(CO)_{12}]$ (*n* = 1, 0.30, 0.22; *n* = 2, 0.30, 0.22), $[AuCl(SC_4H_8)]$ (0.07, 0.22)	[d,e] $[AgAuRu_4(\mu_3\text{-}H)_2\{\mu\text{-}Ph_2P(CH_2)_nPPh_2\}(CO)_{12}]$ (*n* = 1, 0.23 g, 72%; *n* = 2, 0.21 g, 66%)

(*b*) Synthesis of the bimetallic clusters $[M_2Ru_4H_2\{\mu\text{-}Ph_2P(CH_2)_nPPh_2\}(CO)_{12}]$ (M = Ag or Au; *n* = 1 or 2)

Reagents and quantities (g, mmol) used	Product isolated (yield)[a]
$[Cu_2Ru_4(\mu_3\text{-}H)_2\{\mu\text{-}Ph_2P(CH_2)_nPPh_2\}(CO)_{12}]$ (*n* = 1, 0.30, 0.24; *n* = 2, 0.30, 0.24), $[Ag(NCMe)_4]PF_6$ (0.30, 0.72)	[f] $[Ag_2Ru_4(\mu_3\text{-}H)_2\{\mu\text{-}Ph_2P(CH_2)_nPPh_2\}(CO)_{12}]$ (*n* = 1, 0.23 g, 72%; *n* = 2, 0.21 g, 65%)
$[Cu_2Ru_4(\mu_3\text{-}H)_2\{\mu\text{-}Ph_2P(CH_2)_nPPh_2\}(CO)_{12}]$ (*n* = 1, 0.30, 0.24; *n* = 2, 0.30, 0.24), $[AuCl(SC_4H_8)]$ (0.16, 0.50)	[d] $[Au_2Ru_4(\mu_3\text{-}H)(\mu\text{-}H)\{\mu\text{-}Ph_2P(CH_2)_nPPh_2\}(CO)_{12}]$ (*n* = 1, 0.27 g, 74%; *n* = 2, 0.27 g, 74%)
$[Ag_2Ru_4(\mu_3\text{-}H)_2\{\mu\text{-}Ph_2P(CH_2)_nPPh_2\}(CO)_{12}]$ (*n* = 1, 0.30, 0.22; *n* = 2, 0.30, 0.22), $[AuCl(SC_4H_8)]$ (0.16, 0.50)	[d] $[Au_2Ru_4(\mu_3\text{-}H)(\mu\text{-}H)\{\mu\text{-}Ph_2P(CH_2)_nPPh_2\}(CO)_{12}]$ (*n* = 1, 0.25 g; 74%; *n* = 1, 0.24 g, 71%)
$[AgCuRu_4(\mu_3\text{-}H)_2\{\mu\text{-}Ph_2P(CH_2)_nPPh_2\}(CO)_{12}]$ (*n* = 1, 0.20, 0.15; *n* = 2, 0.20, 0.15), $[Ag(NCMe)_4]PF_6$ (0.10, 0.24)	[f] $[Ag_2Ru_4(\mu_3\text{-}H)_2\{\mu\text{-}Ph_2P(CH_2)_nPPh_2\}(CO)_{12}]$ (*n* = 1, 0.14 g, 68%; *n* = 2, 0.15 g, 73%)
$[AuCuRu_4(\mu_3\text{-}H)_2\{\mu\text{-}Ph_2P(CH_2)_nPPh_2\}(CO)_{12}]$ (*n* = 1, 0.21, 0.15; *n* = 2, 0.21, 0.15), $[AuCl(SC_4H_8)]$ (0.05, 0.16)	[d] $[Au_2Ru_4(\mu_3\text{-}H)(\mu\text{-}H)\{\mu\text{-}Ph_2P(CH_2)_nPPh_2\}(CO)_{12}]$ (*n* = 1, 0.17 g, 74%; *n* = 2, 0.15 g, 65%)
$[AgAuRu_4(\mu_3\text{-}H)_2\{\mu\text{-}Ph_2P(CH_2)_nPPh_2\}(CO)_{12}]$ (*n* = 1, 0.21, 0.15; *n* = 2, 0.21, 0.15), $[AuCl(SC_4H_8)]$ (0.05, 0.16)	[d] $[Au_2Ru_4(\mu_3\text{-}H)(\mu\text{-}H)\{\mu\text{-}Ph_2P(CH_2)_nPPh_2\}(CO)_{12}]$ (*n* = 1, 0.16 g, 72%; *n* = 2, 0.15 g, 67%)

[a] Yields are based on the amount of cluster compound taken for reaction. [b] The chromatography was performed on a Florisil column (20 × 3 cm) at −20 °C. [c] The chromatography afforded two red fractions, which contained small amounts of the bimetallic clusters $[Cu_2Ru_4(\mu_3\text{-}H)_2\{\mu\text{-}Ph_2P(CH_2)_nPPh_2\}(CO)_{12}]$ and $[Ag_2Ru_4(\mu_3\text{-}H)_2\{\mu\text{-}Ph_2P(CH_2)_nPPh_2\}(CO)_{12}]$ (*n* = 1 or 2), as well as the main fraction, which contained the trimetallic product. The copper–ruthenium bimetallic cluster was eluted before the trimetallic product and the silver–ruthenium species was eluted afterwards. [d] The chromatography was performed on an alumina column (20 × 3 cm) at ambient temperature. [e] The chromatography afforded a red fraction, which contained a small amount of the bimetallic cluster $[Au_2Ru_4(\mu_3\text{-}H)(\mu\text{-}H)\{\mu\text{-}Ph_2P(CH_2)_nPPh_2\}(CO)_{12}]$ (*n* = 1 or 2), as well as the main fraction, which contained the trimetallic product. The gold–ruthenium bimetallic cluster was eluted before the trimetallic product. [f] The chromatography was performed on an alumina column (20 × 3 cm) at −20 °C.

intermediate between a capped trigonal bipyramid and a capped square-based pyramid by the $Ph_2P(CH_2)_2PPh_2$ ligand in **12**. This distortion occurs *via* an elongation of one of the Au–Ru separations for the gold atom in the site of higher co-ordination number [M(2)] to a distance which is too large for any significant Au–Ru bonding interaction (3.784 and 3.799 Å for the two different crystalline forms of $[Au_2Ru_4(\mu_3\text{-}H)(\mu\text{-}H)(\mu\text{-}Ph_2PCH_2PPh_2)(CO)_{12}]$[19] **11** and 3.446 Å for $[Au_2Ru_4(\mu_3\text{-}H)(\mu\text{-}H)\{\mu\text{-}Ph_2P(CH_2)_2PPh_2\}(CO)_{12}]$ **12**[11]) (*e.g.* Fig. 2). Clearly, no distortion of this type occurs for the trimetallic clusters **7**–**10**, in which the gold atoms occupy the site of lower co-ordination number [M(1)]. Therefore, it seems that the distortions away from the normal capped trigonal-bipyramidal metal core geometry, which are observed for the bimetallic gold clusters **11** and **12**,[11] are caused by the fact that the site M(2) is occupied by a gold atom rather than by the presence of a gold atom in the site M(1).

Although there is a plane of symmetry through the metal skeleton of each of **5**–**10** [*e.g.* Au, Cu, Ru(1) and Ru(2) in Fig. 1], the conformations adopted by the methylene backbones of the $Ph_2P(CH_2)_nPPh_2$ (*n* = 1 or 2) ligands in the ground state structure of these clusters render the two hydrido ligands inequivalent (*e.g.* Fig. 1). However, only one high-field hydrido ligand resonance is observed in the ^1H NMR spectrum of each cluster at ambient temperature. Thus, **5**–**10** all undergo some dynamic process, which renders the hydrido ligands equivalent, at ambient temperature in solution. Dynamic behaviour involving conformational changes in the methylene backbones of bidentate diphosphine ligands has been previously postulated[20] to explain the similar observations made for the analogous bimetallic clusters $[M_2Ru_4(\mu_3\text{-}H)_2\{\mu\text{-}Ph_2P(CH_2)_nPPh_2\}(CO)_{12}]$ (M = Cu, *n* = 1–6; M = Ag, *n* = 2–6) and it seems very likely that the same process renders the two hydrido ligands equivalent in each of the clusters **5**–**10**. Interestingly, there is only one hydrido ligand resonance in the ^1H NMR spectrum of each of the $Ph_2PCH_2PPh_2$-ligated species **5**, **7** and **9**, even at −100 °C, whereas two signals, which are consistent with the ground-state structure, are observed in the ^1H NMR spectrum of each of the $Ph_2P(CH_2)_2PPh_2$-containing species **6**, **8** and **10** at −100 °C. Thus, the magnitudes of the free energy of activation ($\Delta G^\ddagger$) for the dynamic process are larger for the $Ph_2P(CH_2)_2PPh_2$-ligated clusters. This observation is consistent with the trends in the values of $\Delta G^\ddagger$ previously reported[20] for the same dynamic process in the analogous copper-containing bimetallic clusters **1** and **2** and in the closely related species $[Cu_2Ru_4(\mu_3\text{-}H)_2\{\mu\text{-}Ph_2As(CH_2)_nPPh_2\}(CO)_{12}]$ (*n* = 1 or 2).

Experimental

The clusters $[M_2Ru_4(\mu_3\text{-}H)_2\{\mu\text{-}Ph_2P(CH_2)_nPPh_2\}(CO)_{12}]$ (M = Cu or Ag, *n* = 1 or 2)[8] and the complex $[AuCl(SC_4H_8)]$[21] were prepared as previously described. An adaptation of a published route[22] was utilized to synthesise the complex $[Ag(NCMe)_4]PF_6$. The techniques used and the instrumentation employed for spectroscopic characterization have been described elsewhere.[10] Light petroleum refers to that fraction of b.p. 40–60 °C. Analytical and physical data for the new Group IB metal cluster compounds are presented in Table 1, together with their IR spectra. Table 2 summarizes the results of NMR spectroscopic measurements.

Synthesis of the Trimetallic Cluster Compounds $[MM'Ru_4(\mu_3\text{-}H)_2\{\mu\text{-}Ph_2P(CH_2)_2PPh_2\}(CO)_{12}]$ (M = Cu, M′ = Ag *or* Au; M = Ag, M′ = Au; *n* = 1 *or* 2).—Using the quantities listed in Table 4, a dichloromethane solution (50 cm³) of the appropriate mononuclear complex $[Ag(NCMe)_4]PF_6$ or $[AuCl(SC_4H_8)]$ was added dropwise to a stirred dichloromethane (100 cm³)

Table 5 Fractional atomic coordinates, with estimated standard deviations in parentheses, for $[AuCuRu_4(\mu_3\text{-}H)_2\{\mu\text{-}Ph_2P(CH_2)_2PPh_2\}(CO)_{12}]$ **8**

Atom	*x*	*y*	*z*
Au	0.0296(5)	−0.0677(5)	0.1057(5)
Cu	0.2373(6)	−0.0040(6)	0.1278(5)
Ru(1)	0.3590(6)	0.0577(5)	0.2620(6)
Ru(2)	0.2186(6)	0.1119(5)	0.3403(6)
Ru(3)	0.1482(6)	0.0886(5)	0.1425(6)
Ru(4)	0.1651(6)	0.0154(6)	0.3010(6)
P(1)	−0.0533(9)	−0.0596(9)	0.0291(8)
P(2)	0.2315(9)	−0.0538(9)	0.0140(8)
C(11)	0.4234(10)	0.0564(12)	0.4214(10)
O(11)	0.5098(10)	0.0356(13)	0.5193(10)
C(12)	0.4406(10)	0.0048(10)	0.2117(10)
O(12)	0.5217(10)	−0.0262(13)	0.1737(10)
C(13)	0.4206(10)	0.1098(13)	0.2343(10)
O(13)	0.4803(10)	0.1389(12)	0.2393(10)
C(21)	0.2613(10)	0.1715(14)	0.3261(10)
O(21)	0.2700(10)	0.1993(14)	0.3817(10)
C(22)	0.1231(10)	0.1308(13)	0.3735(10)
O(22)	0.0080(10)	0.1595(12)	0.3528(10)
C(23)	0.2741(10)	0.0877(10)	0.4434(10)
O(23)	0.3192(14)	0.0993(14)	0.5512(10)
C(31)	−0.0473(10)	0.1091(10)	0.1541(10)
O(31)	−0.1269(10)	0.1326(13)	0.1263(10)
C(32)	0.0746(10)	0.0569(12)	−0.0036(10)
O(32)	0.1231(10)	0.0840(12)	−0.0633(10)
C(33)	0.1729(10)	0.1607(10)	0.1045(10)
O(33)	0.2331(12)	0.1925(13)	0.1593(12)
C(41)	0.2180(12)	0.0159(12)	0.4282(12)
O(41)	0.2589(13)	−0.0109(11)	0.5202(13)
C(42)	0.1300(12)	0.9502(12)	0.2762(12)
O(42)	0.1094(13)	−0.0977(12)	0.2759(13)
C(43)	0.0087(12)	0.0438(13)	0.3277(12)
O(43)	−0.0756(12)	0.0523(13)	0.3284(12)
C(1)	0.0219(12)	−0.1228(12)	−0.0265(12)
C(2)	0.1173(12)	−0.0879(12)	−0.0710(12)
C(14)	−0.1540(13)	−0.0294(10)	−0.0930(12)
C(15)	−0.1578(13)	−0.0573(10)	−0.1783(12)
C(16)	−0.2200(13)	−0.0415(10)	−0.2706(12)
C(17)	−0.2784(13)	0.0021(10)	−0.2776(12)
C(18)	−0.2745(13)	0.0299(10)	−0.1922(12)
C(19)	−0.2124(13)	0.0141(10)	−0.1000(12)
C(24)	−0.1386(11)	−0.0998(10)	0.1547(11)
C(25)	−0.2350(11)	−0.0787(10)	0.1156(11)
C(26)	−0.3033(11)	−0.1049(10)	0.1619(11)
C(27)	−0.2753(11)	−0.1521(10)	0.1968(11)
C(28)	−0.1790(11)	−0.1732(10)	0.1853(11)
C(29)	−0.1106(11)	−0.1470(10)	0.1390(11)
C(34)	0.3336(12)	−0.1114(12)	0.1041(11)
C(35)	0.3786(12)	−0.1160(12)	0.0524(11)
C(36)	0.4338(12)	−0.1586(12)	0.1925(11)
C(37)	0.4442(12)	−0.1965(12)	0.1282(11)
C(38)	0.3992(12)	−0.1919(12)	0.0260(11)
C(39)	0.3439(12)	−0.1493(12)	−0.0119(11)
C(44)	0.3178(12)	−0.0397(13)	−0.0850(13)
C(45)	0.2589(12)	−0.0101(12)	−0.1614(12)
C(46)	0.3088(13)	0.0089(13)	−0.2326(12)
C(47)	0.4176(12)	−0.0016(13)	−0.2274(12)
C(48)	0.4765(12)	−0.0312(13)	−0.1510(12)
C(49)	0.4266(12)	−0.0503(13)	−0.0798(12)

solution of the bimetallic cluster compound over a period of 1 h. After removal of the solvent under reduced pressure, the crude residue was dissolved in a dichloromethane–light petroleum (1:2) mixture. Chromatography, using the appropriate conditions (Table 4) and eluting with a dichloromethane–light petroleum (1:2) mixture, afforded a red fraction containing the trimetallic cluster compound $[MM'Ru_4(\mu_3\text{-}H)_2\{\mu\text{-}Ph_2P(CH_2)_nPPh_2\}(CO)_{12}]$ (M = Cu, M′ = Ag or Au; M = Ag, M′ = Au; *n* = 1 or 2). Fractions containing small amounts of bimetallic clusters in which both Group IB metals had been exchanged were also obtained from the chromatography and details are given in Table 4. After removal of the solvent from the fraction containing the trimetallic species, crystallization of the residue from dichloromethane–light petroleum afforded red *microcrystals* of the product. Table 4 lists the yields obtained.

Synthesis of the Bimetallic Cluster Compounds $[M_2Ru_4H_2\{\mu\text{-}Ph_2P(CH_2)_nPPh_2\}(CO)_{12}]$ (M = Ag *or* Au, *n* = 1 *or* 2) *via Group IB Metal Exchange Reactions*.—Using the quantities listed in Table 4, a dichloromethane (50 cm^3) solution of the bimetallic or trimetallic cluster compound was treated with a dichloromethane (50 cm^3) solution containing the appropriate mononuclear complex $[Ag(NCMe)_4]PF_6$ or $[AuCl(SC_4H_8)]$ and the mixture was stirred for 15 min. After removal of the solvent under reduced pressure, the crude residue was dissolved in a dichloromethane–light petroleum (2:3) mixture. Chromatography, using the appropriate conditions (Table 4) and eluting with a dichloromethane–light petroleum (2:3) mixture, afforded one red fraction. After removal of the solvent from this fraction under reduced pressure, crystallization of the residue from a dichloromethane–light petroleum mixture afforded red *microcrystals* of the bimetallic cluster compound $[M_2Ru_4H_2\{\mu\text{-}Ph_2P(CH_2)_nPPh_2\}(CO)_{12}]$ (M = Ag or Au; *n* = 1 or 2). Table 4 lists the yields obtained. The ^1H and $^{31}P\text{-}\{^1H\}$ NMR and IR spectra of samples of the bimetallic species synthesised in the above manner are identical to the data quoted in the literature.[8,9,11]

Crystal Structure Determination for **8**.—Suitable crystals of **8** were grown from a dichloromethane–diethyl ether–light petroleum mixture by slow layer diffusion at −20 °C.

Crystal data for **8**. $C_{38}H_{26}AuCuO_{12}P_2Ru_4$, *M* = 1401.06, monoclinic, space group $P2_1/c$, $a = 12.668(2)$, $b = 27.383(3)$, $c = 13.828(2)$ Å, $\beta = 104.122(2)°$, $U = 4659.14$ Å^3, $F(000) = 2656$, μ(Mo-Kα) = 47.40 cm^{-1}, $Z = 4$, $D_c = 2.10$ g cm^{-3}.

Data collection. The methods of data collection and data processing used for **8** were similar to those described previously.[23] The crystal selected for data collection had dimensions of 0.25 × 0.22 × 0.13 mm. A scan width of 0.8° in θ was used to collect data in the θ range 3–25° by the ω–2θ technique. Equivalent reflections were merged to give 4467 data with $I/\sigma(I) > 3.0$. No absorption corrections were applied to the data set.

Structure solution and refinement. The positions of the metal atoms in the structure of **8** were deduced from a Patterson synthesis. The remaining non-hydrogen atoms were found from subsequent Fourier-difference syntheses. The positions of the two μ_3-hydrido ligands were derived from suitable potential energy minimization calculations.[24] During the final stages of refinement,[25] anisotropic thermal parameters were assigned to the metal and phosphorus atoms.

Full-matrix refinement of the atomic, positional, and thermal parameters for **8** converged at final *R* and *R′* values of 0.0605 and 0.0603, respectively, with weights of $w = 1/\sigma^2(F_o)$ assigned to individual reflections. The phenyl rings in the structure of **8** were treated as rigid hexagons [*d*(C–C) 1.395, *d*(C–H) 1.08 Å], with fixed thermal parameters of 0.08 Å^2 assigned to the H atoms of each ring. The final atomic coordinates for compound **8** are listed in Table 5.

Additional material available from the Cambridge Crystallographic Data Centre comprises thermal parameters and remaining bond lengths and angles.

Acknowledgements

We thank the Royal Society and the SERC for a studentship (to

S. S. D. B.) and Johnson Matthey for a generous loan of gold, silver, and ruthenium salts.

References

1 Part 15, C. J. Brown, P. J. McCarthy and I. D. Salter, *J. Chem. Soc., Dalton Trans.*, 1990, 3583.

2 See, for example, I. D. Salter, *Adv. Organomet. Chem.*, 1989, **29**, 249 and refs. therein.

3 See, for example, K. P. Hall and D. M. P. Mingos, *Prog. Inorg. Chem.*, 1984, **32**, 237; P. Braunstein and J. Rose, *Gold Bull.*, 1985, **18**, 17 and refs. therein.

4 See, for example, D. A. Roberts and G. L. Geoffroy, in *Comprehensive Organometallic Chemistry*, eds. G. Wilkinson, F. G. A. Stone and E. W. Abel, Pergamon, Oxford, 1982, ch. 40 and refs. therein.

5 I. D. Salter, *J. Organomet. Chem.*, 1985, **295**, C17.

6 M. J. Freeman, A. G. Orpen and I. D. Salter, *J. Chem. Soc., Dalton Trans.*, 1987, 1001.

7 S. R. Drake, B. F. G. Johnson and J. Lewis, *J. Chem. Soc., Dalton Trans.*, 1989, 505.

8 S. S. D. Brown, I. D. Salter and L. Toupet, *J. Chem. Soc., Dalton Trans.*, 1988, 757.

9 S. S. D. Brown, I. D. Salter, D. B. Dyson, R. V. Parish, P. A. Bates and M. B. Hursthouse, *J. Chem. Soc., Dalton Trans.*, 1988, 1795.

10 S. S. D. Brown, P. J. McCarthy, I. D. Salter, P. A. Bates, M. B. Hursthouse, I. J. Colquhoun, W. McFarlane and M. Murray, *J. Chem. Soc., Dalton Trans.*, 1988, 2787.

11 S. S. D. Brown, I. D. Salter, A. J. Dent, G. F. M. Kitchen, A. G. Orpen, P. A. Bates and M. B. Hursthouse, *J. Chem. Soc., Dalton Trans.*, 1989, 1227.

12 S. S. D. Brown and I. D. Salter, *J. Organomet. Chem.*, 1989, **377**, C31.

13 S. S. D. Brown, I. D. Salter and B. M. Smith, *J. Chem. Soc., Chem. Commun.*, 1985, 1439.

14 I. D. Salter, unpublished work.

15 S. S. D. Brown, I. D. Salter, V. Sik, I. J. Colquhoun, W. McFarlane, P. A. Bates, M. B. Hursthouse and M. Murray, *J. Chem. Soc., Dalton Trans.*, 1988, 2177.

16 P. J. McCarthy, I. D. Salter and V. Sik, *J. Organomet. Chem.*, 1988, **344**, 411.

17 M. J. Freeman, A. G. Orpen and I. D. Salter, *J. Chem. Soc., Dalton Trans.*, 1987, 379.

18 C. J. Brown, P. J. McCarthy, I. D. Salter, K. P. Armstrong, M. McPartlin and H. R. Powell, *J. Organomet. Chem.*, 1990, **394**, 711.

19 A. G. Orpen and I. D. Salter, *Organometallics*, 1991, **10**, 111.

20 C. P. Blaxill, S. S. D. Brown, J. C. Frankland, I. D. Salter and V. Sik, *J. Chem. Soc., Dalton Trans.*, 1989, 2039.

21 R. Uson and A. Laguna, *Organomet. Synth.*, 1986, **3**, 324.

22 G. J. Kubas, *Inorg. Synth.*, 1979, **19**, 90; S. S. D. Brown and I. D. Salter, *Organomet. Synth.*, 1986, **3**, 315.

23 P. F. Jackson, B. F. G. Johnson, J. Lewis, W. J. H. Nelson and M. McPartlin, *J. Chem. Soc., Dalton Trans.*, 1982, 2099.

24 A. G. Orpen, *J. Chem. Soc., Dalton Trans.*, 1980, 2509.

25 G. M. Sheldrick, SHELX 76 crystal structure solving package, University of Cambridge, 1976.

Received 13*th July* 1992; *Paper* 2/03682G